Photogrammetric Assessment of Flexure Induced Cracking of Reinforced Concrete Beams under Service Loads

Pease, Bradley Justin; Geiker, Mette Rica; Stang, Henrik; Weiss, Jason

Published in:
Proceedings of the Second International RILEM Symposium

Publication date:
2006

Document Version
Publisher's PDF, also known as Version of record

PHOTOGRAMMETRIC ASSESSMENT OF FLEXURE INDUCED CRACKING IN REINFORCED CONCRETE BEAMS UNDER SERVICE LOADS

Brad J. Pease [(1)], Mette R. Geiker [(1)], Henrik Stang [(1)], and W. Jason Weiss [(2)]

(1) Department of Civil Engineering (BYG•DTU), Technical University of Denmark, Denmark

(2) School of Civil Engineering, Purdue University, USA

Abstract ID Number (given by the scientific editors/organizers): ……..153

Keywords: Reinforced Concrete, Cracking, Photogrammetry, Flexural Load, Crack Width

Author contacts

Authors	E-Mail	Fax	Postal address
Brad J. Pease	bjp@byg.dtu.dk	+45 4588 3282	DTU – Bygning 118
Mette R. Geiker	mge@byg.dtu.dk	+45 4588 3282	Brovej
Henrik Stang	hs@byg.dtu.dk	+45 4588 3282	DK – 2800 Kgs. Lyngby
W. Jason Weiss	wjweiss@ecn.purdue.edu	+1-765-496-1364	School of Civil Engineering 550 Stadium Mall Drive West Lafayette, IN 47907

Contact person for the paper: Brad J. Pease

Presenter of the paper during the Conference: Brad J. Pease

Total number of pages of the paper (the first pages and the licence to publish excluded): 11

PUBLICATION AGREEMENT REF: ……..153

The corresponding undersigned author submitted an article untitled CRACKING BEHAVIOR OF REINFORCED CONCRETE BEAMS UNDER SERVICE LOADS

for publication in

1. RILEM journal: Materials and Structures
2. Conference presentation (short title, date and city): Advances in Concrete through Science and Engineering, Sept. 11-13, 2006, Quebec City, Canada
3. Book, technical report (Ref. or title): …….
4. Other type of publication (please complete): ……...……..

Authored by (listed in order for each author, with Surname + Initial given name): Pease, B., Geiker, M., Stang, H., and Weiss, J.

The copyright to this article is transferred to RILEM (for U.S. government employees: to the extent transferable) effective if and when the article is accepted for publication. The copyright transfer covers the exclusive right to reproduce and distribute the article, including reprints, translations, photographic reproductions, microform, electronic form (offline, online) or any other reproductions of similar nature.

The corresponding author warrants that:

- this contribution is not under consideration for publication elsewhere
- the work described has not been published before (except in form of an abstract or as part of a published lecture, review or thesis)
- it does not contain any libelous or unlawful statements, and that it does not infringe on others' rights. Each author is responsible for all statements made in the article.
- this article will not be distributed in print during the period of submission to publication
- its publication has been approved by all co-authors, if any, as well as – tacitly or explicitly – by the responsible authorities at the institution where the work was carried out.
- he/she has full power to make this grant. The corresponding author signs for and accepts responsibility for releasing this material on behalf of any and all co-authors.
- After submission of this agreement signed by the corresponding author, changes of authorship or in the order of the authors listed will not be accepted by RILEM.

Permission must be obtained to reprint or adapt a table or figure; to reprint quotations exceeding the limits of fair use from one source. Authors must write to the original author(s) and publisher to request nonexclusive world rights in all languages to use copyrighted material in the present article and in future print and non print editions. Authors are responsible for obtaining proper permission from copyright owners and are liable for any and all licensing fees required. Authors must include copies of all permissions and credit lines with the article submission.

Each author retains the following rights:

- All proprietary rights, other than copyright.
- The right to make copies of all or part of the material for use by the author in teaching, provided these copies are not offered for sale.
- The right to make copies of the work for circulation within an institution that employs the author.
- The right to make oral presentations of the material.
- The right to self-archive an author-created version of his/her article on his/her own website and his/her institution's repository, including his/her final version; however he/she may not use the publisher's PDF version which is posted on the publisher's website. Furthermore, the author may only post his/her version provided acknowledgement is given to the original source of publication and a link is inserted to the published article on the publisher's website. The link must be accompanied by the following text: "The original publication is available at the publisher's web site" (precise URL will be given for each type of published article). The author must also post a statement that the article is accepted for publication, that it is copyrighted by RILEM, and that readers must contact RILEM for permission to reprint or use the material in any form.
- The right to use all or part of the published material in any book by the author, provided that a citation to the article is included and written permission from the publisher is obtained.

Each author agrees that all dissemination of material under the conditions listed above will include credit to RILEM as the copyright holder.

In the case of works prepared under U.S. Government contract, the U.S. Government may reproduce, royalty-free, all or part of the material and may authorize others to do so, for official U.S. Government purposes only, if so required by the contract.

The authors must use for their accepted article, the appropriate DOI (Digital Object Identifier) when available (after receipt of the final version by the publisher). Articles disseminated via RILEM web sites (and sub-contractors' web sites if any) are indexed, abstracted, and referenced by Google Search, Google Scholar, Google Print and SWOC (Swets online Content).

Date: ……..

Corresponding **author's hand-written signature**: Corresponding author's name: Brad J. Pease

PHOTOGRAMMETRIC ASSESSMENT OF FLEXURE INDUCED CRACKING OF REINFORCED CONCRETE BEAMS UNDER SERVICE LOADS

Brad J. Pease (1), Mette R. Geiker (1), Henrik Stang (1), and W. Jason Weiss (2)

(1) Department of Civil Engineering, Technical University of Denmark, Denmark

(2) School of Civil Engineering, Purdue University, USA

Abstract

Reinforced concrete structures are known to crack due to restrained shrinkage, temperature gradients, application of load, and expansive reactions. Cracks provide paths for rapid ingress of moisture, chlorides, and other aggressive substances, which may affect the long-term durability of the structure. For example, concrete cracks which reach the reinforcing steel may contribute to rapid corrosion initiation and propagation. Previous research has shown that cracked reinforced concrete under static flexural loading may have an increased ingress of chloride ions along the reinforcement/concrete interface.

The aim of this paper is to provide a detailed description of the development of cracks in reinforced concrete under flexural load. Cracking at both realistic service load levels (1.0-1.8 times estimated cracking load) and unrealistically high service load levels (> 0.5 times beam capacity) has been investigated. These load levels result in relatively small cracks (< ~0.1 mm) and cracks larger than expected in field concrete, respectively. The investigation constitutes a preliminary study in a project aimed at describing the effect of cracking on the transport and corrosion behaviors of reinforced concrete.

Reinforced concrete beams were subjected to flexural load and the associated cracking behavior was monitored using three dimensional photogrammetry. The results indicate that minute surface cracks (~10 microns) may cause slip and separation at the reinforcement/concrete interface. This has direct implications on the ingress and corrosion behaviors in concrete subjected to flexural loading, e.g. samples prepared for laboratory studies.

1. INTRODUCTION

A U.S. Federal Highway Administration report estimates the total cost to repair or replace that nation's structurally deficient concrete bridges to be between $78 billion and $112 billion [1]. Furthermore, the estimated average cost to simply maintain a constant number and distribution of deficient bridges was placed at $5.2 billion annually between 2001 and 2011 [2]. These estimates only account for a single structural application of reinforced concrete in one country; however, they alone indicate necessity for control of corrosion in reinforced concrete.

Concrete frequently cracks under even minimal tensile loading (when compared to compressive loading causing crack formation), which may be induced via restrained hygral/thermal shrinkage or by mechanical load. Cracking allows for increased local ingress of substances contributing to corrosion (i.e., chlorides, carbon dioxide, oxygen) near the crack surfaces [3-10]. Permeability increases with crack width and appears to have a dependence on the material type, i.e. paste, mortar, or concrete [3,4]. Results from Aldea et al. [4] indicate that alterations in mixture proportions, such as aggregate content/size and water-to-cement ratio (w/c), may affect crack morphology and the permeability of the cracked material. Expressions for an influence factor of cracks on diffusion of chlorides were developed and showed reasonable correlation with field measurements; however, the investigations did only cover idealized and relatively large cracks (crack width, $w \geq 0.2$ mm) [5]. These expressions indicate diffusion is significantly influenced by cracks width less than 0.2 mm. Similarly, Rodriquez and Hooton [6] have shown that load induced cracks with widths greater than 80 μm act as free surfaces for diffusion of chloride ions. Under specific conditions autogenous (self) healing occurs, which may provide a reduction in chloride migration (28-35% of migration in newly cracked specimen) and improved (reduced) permeability, despite only a minor recovery of mechanical performance [7,8]. In contrast, cyclic loading resulting in the opening and closing of concrete cracks may result in increased chloride ingress [9]; although the importance of this type of loading in structural applications should be further assessed. Finally, results have shown a preferential ingress of chlorides along the reinforcement/concrete interface in cracked concrete [10]. This ingress behavior may affect reinforcement corrosion, specifically anode and cathode size, significantly.

The use of low water-to-cement ratios (w/c) and certain mineral admixtures, such as silica fume, in so-called high performance concrete has resulted in concretes with improved strength, low permeability, and increased electrical resistance. In optimum conditions (i.e., without cracks), such concretes provide a highly protective barrier to ingress. However, these concretes are especially susceptible to early-age cracking [11] due to increases in autogenous shrinkage, material stiffness, and brittleness in conjunction with reduced creep [12]. Field observations support these experimental conclusions as cracking has increased in reinforced concrete bridge decks in recent years [13].

If cracks in reinforced concrete intersect the reinforcement a local depassivation of the steel may occur, and due to the increased ingress behavior a localized corrosion may rapidly initiate. Several studies exist on the effect of cracks on reinforcement corrosion [14-18]. Investigations on uncracked and cracked (with widths between 0.1 mm and 0.7 mm) reinforced concrete showed that crack widths of 0.1 mm, dependent on the w/c and cover, may affect the time to corrosion initiation [14,15]. Concrete with crack widths greater than

0.1 mm allowed corrosion to initiate nearly immediately when exposed to chloride solution. The effect of crack width on the rate of corrosion was found to diminish over time [14]. This suggests that crack parameters effect corrosion initiation more than propagation.

Thus, previous studies [3-10,14-16] indicate that ingress and corrosion behaviors are strongly influenced by crack width and morphology; however, minimal work has been carried out to compare cracks in these experimental investigations with in-situ cracks. These investigations have utilized various methods including splitting tensile loading, direct tensile loading, flexural loading, freeze-thaw cycling, and the use of shims to produce cracks with widths varying between 0.08 mm to 0.70 mm. Limited information has been published concerning cracking of field concrete; however, an investigation of various pavements in Indiana indicates that in-situ cracks may be relatively small compared to the range used in these experiments (even after 25 years of traffic and environmental loading) [19]. Additionally, several studies have used segments of reinforcement to monitor the effect of cracks on corrosion [14-16]. While these studies have provided important insight into the effect of cracks on reinforcement corrosion, the segments are not mechanically accurate which may affect the cracking, ingress, and corrosion behaviors.

The aim of this paper is to investigate the cracking behavior of laboratory specimen which will be used in an investigation of the effect cracks have on ingress and corrosion. In particular emphasis has been placed on developing an experimental technique which allows detailed information about cracking patterns and geometry to be obtained. Such data is critical for development of models for the effect of cracking on transport, corrosion initiation, and corrosion development. Finally, this initial investigation will facilitate comparison with in-situ cracking in future work.

2. RESEARCH SIGNIFICANCE

Cracking in reinforced concrete allows for rapid ingress of chlorides and other deleterious substances which may initiate corrosion of reinforcement. In order to investigate the effect of cracks on ingress and corrosion in laboratory conditions, researchers often use flexural loading. The flexural load-induced cracks may not however accurately represent in-situ cracking. Variation in crack parameters (i.e., width, tortuosity) may result in varying ingress and corrosion behavior. Therefore, a comparison between cracking in a laboratory specimen, designed for a corrosion investigation, and in-situ cracking is needed. This paper presents results of photogrammetric analysis of cracks in laboratory specimen, which will be compared to petrographic analysis and in-situ cracks in subsequent work.

3. EXPERIMENTAL PROCEDURE

3.1 Specimen preparation and mixture design

Reinforced concrete beams with dimensions 150 mm x 150 mm x 600 mm were cast with two 8 mm diameter deformed bar reinforcement, as shown in Figure 1. The mixture designs used, described in Table 1, contained sea sand, and two naturally rounded coarse aggregates with maximum aggregate sizes of 8 mm and 16 mm, respectively. White Portland cement from Aalborg Portland, Denmark, was used in all mixtures. The beams were cast with the reinforcement near the bottom of the form to reduce the effect of bleeding on the transition zone. The specimen were cast in three layers, vibrated, and finished using a steel trowel. The beams remained in the forms for 24 hours at 20°C, were demolded and placed in water

saturated with lime at 20°C for an additional 55 days. Three cylinders for each mixture were cast and cured under identical conditions for 28 days for standard compressive strength measurements.

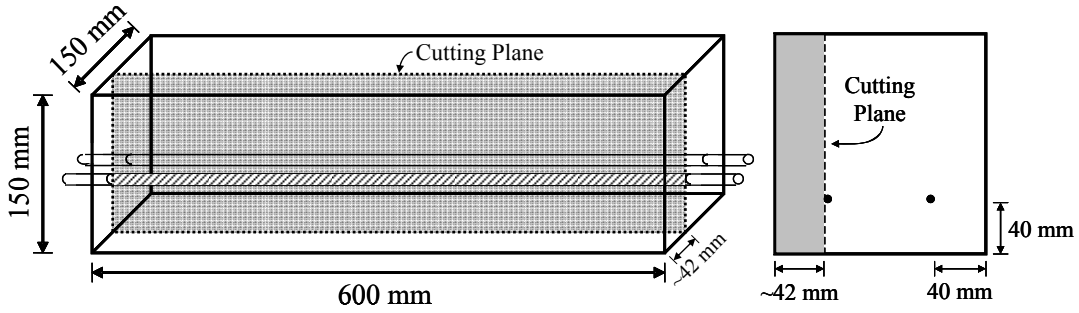

Figure 1: Specimen Geometry with Location of Saw Cutting Indicated.

After removal from the lime saturated water a concrete saw was used to cut the covering concrete from one side of the reinforced concrete beams (see Figure 1) to expose the reinforcement. Approximately 2 mm of the 8 mm diameter reinforcing bar was cut away to provide a view of the reinforcement. Figure 2(a) shows an example of one of the beams after saw cutting where it is possible to see both the concrete and reinforcing steel. Following saw cutting the surfaces of the concrete and steel were further prepared to allow for three dimensional (3-D) photogrammetry analysis of cracking at the interface. Further details on the surface preparation necessary for 3-D photogrammetry are provided in Section 3.2. After saw cutting and surface preparation for photogrammetry the samples were stored sealed in plastic until testing.

Table 1: Mixture Proportions, Compressive Strength, and Beam Failure Load

Mix Design	w/c	Cement Content	Sea Sand	4-8 mm	8-16 mm	f'c	Beam Failure Load
	-	kg/m^3 (lb/yd^3)	kg/m^3 (lb/yd^3)	kg/m^3 (lb/yd^3)	kg/m^3 (lb/yd^3)	MPa (psi)	kN (kips)
1	0.50	330 (556)	809 (1363)	1073 (1808)	-	43 (6200)	52.2 (11.7)
2	0.50	330 (556)	766 (1291)	150 (252)	953 (1606)	39 (5700)	54.9 (12.3)

3.2 Testing procedures

Two test series were preformed by applying varying loads in three point bending over a span length of 500 mm. 3-D photogrammetry measurements, which are discussed further in the following section, were taken for both test series. Series I involved testing of one specimen from each mixture. In the initial test series an increasing load level was applied to a single specimen to assess which loads were of interest for further analysis. The estimated cracking loads of the cut specimen, determined using the ACI Building Code, were found to be 13.6 kN and 13.0 kN for the 8 mm and 16 mm maximum aggregate size specimen, respectively. The specimen was loaded to multiples of the estimated cracking load including 1.0, 1.2, 1.4, 1.6, and 1.8. Additionally, the beams were loaded to 30.0 kN and 35.0 kN to investigate cracking under more extreme loading conditions. Load was applied at a constant rate for three minutes to the maximum load followed by unloading over the same amount of time. The beams used for the Series I were then loaded to failure, however photogrammetry measurements were not taken due to danger of damage to the equipment. It should be noted

that previous cracking of specimens caused stiffness reductions affecting the crack opening response, necessitating Series II testing on previously unloaded samples to determine the actual cracking response. Thus, based upon the Series I results additional measurements were taken for Series II, on uncracked samples, at load levels including 1.4 and 1.8 times the estimated cracking load and at 35.0 kN.

3.3 3-D photogrammetry setup

A commercially available 3-D photogrammetry system was utilized to provide quantitative and qualitative information on the cracking behavior in the specimen. In order to facilitate photogrammetry measurements adequate contrast in the grayscale of individual objects is required. This was achieved by using black and white spray paint to apply a stochastic spatter pattern as seen in Figure 2(b). The individual aggregates remained clearly visible through the black and white spatter pattern. The surface of the reinforcement was also painted white to eliminate reflection of light from the polished steel.

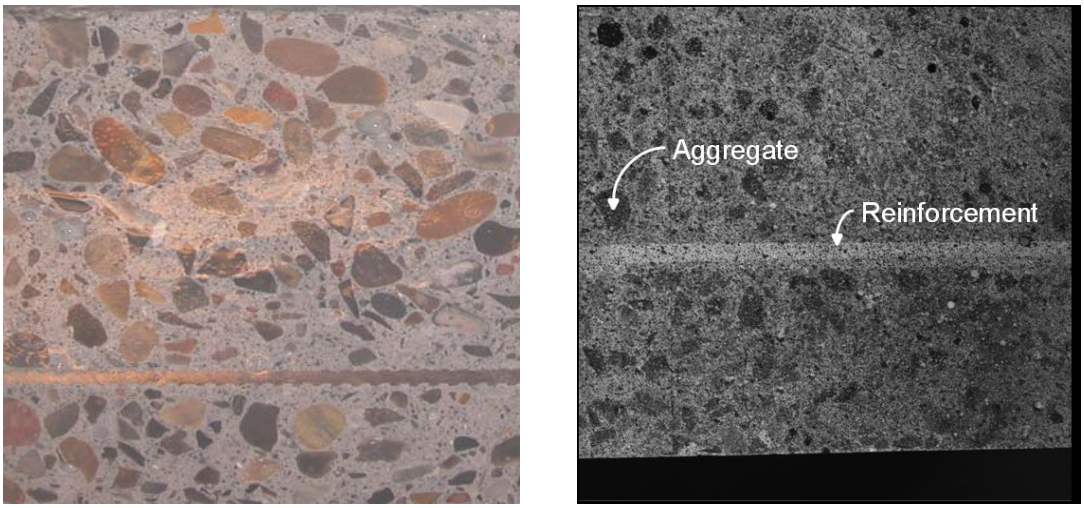

(a) (b)

Figure 2: Specimen Surface after Saw Cutting with Exposed Reinforcement (a) prior to and (b) after Application of Spatter Pattern.

The photogrammetry system uses two charged couple device (CCD) digital cameras to capture images at a predefined interval, once every second during testing in this case. The two CCD cameras were positioned at the same height and were focused on the same surface, but from different angles. The individual cameras will be referred to as camera right and camera left in the following explanation. A calibration is preformed prior to testing, using a calibration plate provided by the manufacturer, in order to insure accurate measurements. At each image capture interval, or stage an image from both cameras was taken. Figure 2(b) shows an image from one of the cameras, which were focused on a 100 mm x 100 mm area at the tension face directly opposite the applied load in order to monitor cracking. Based on the manufacture's specification an accurate of $1x10^{-5}$ times the image dimension (or 1 μm for the specimens used here) is possible for this equipment. A comparison of crack widths measured using the photogrammetry equipment and an extensiometer clip gage showed reasonable

accuracy (±5 μm). In order to calculate strain and displacement in the reinforced concrete beams a computational mask is applied by the provided software to the initial, non-deformed specimen surface image from camera left, see Figure 3(a). The mask consists of 15 x 15 pixel facets which overlap by two pixels, corresponding to length units of approximately 0.7 mm x 0.7 mm and 0.1 mm, respectively. The software then associates individual facets with the grayscale image contained within. Next, the software 'finds' the corresponding facets in the initial, non-deformed camera right image by searching for the same grayscale images. The software then tracks the deformation of the individual facets as load is applied. Figure 3(b) depicts the deformed computational mask after loading and cracking of a specimen. The discontinuity introduced by the crack in Figure 3(b) causes some facets to be lost as the software is unable to locate the appropriate grayscale images. The 2-D coordinates of the individual facets from the right and left camera images are determined and photogrammetric techniques are used to calculate 3-D movements. Using this, strain is calculated and visualized and point-point displacements are may be determined at any point on the measured surface. Additional information on the photogrammetry equipment, software, and the techniques employed therein can be found elsewhere [20].

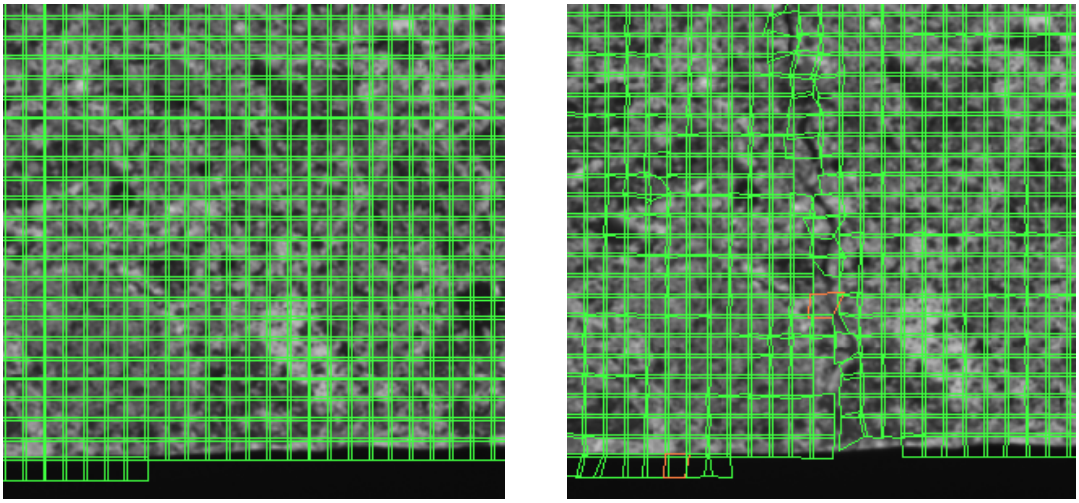

(a) (b)

Figure 3: Specimen Surface with Computational Mask Applied over the (a) Non-Deformed Specimen (Initial Stage) and (b) Deformed Specimen (Images are Zoomed).

4. RESULTS

A computational mask, as shown in Figure 3 is utilized to compute major strain in individual facets. This calculated strain is visualized using a color spectrum (similar to finite element analysis) and overlaid on an image of the specimen surface as shown in Figure 4. The strain overlay however contains holes where strain computations were not possible. These holes may be caused by inadequate contrast in grayscale, which is easily corrected by applying additional paint spatter before loading, or by inconsistent images from the two camera angles. The latter presents a problem for cut concrete surfaces due to the presence of large air voids. Voids, when viewed from different angles, vary visually due to changes in the line of sight. The larger voids were filled with paraffin wax to allow strain computations, however some

voids remained. The strain is computed based upon the deformation in the computational mask as opposed to strain in the actual material. Therefore, Figure 4 shows excessive strain at the crack surface, which is inaccurate in terms of actual material behavior as the presence of a crack would relieve strain locally. This erroneous representation is explained by Figure 3(b) which shows the facets directly next to the crack are substantially deformed after cracking of the concrete. However with this flaw, the computed strains provide useful qualitative information on the cracking behavior in reinforced concrete.

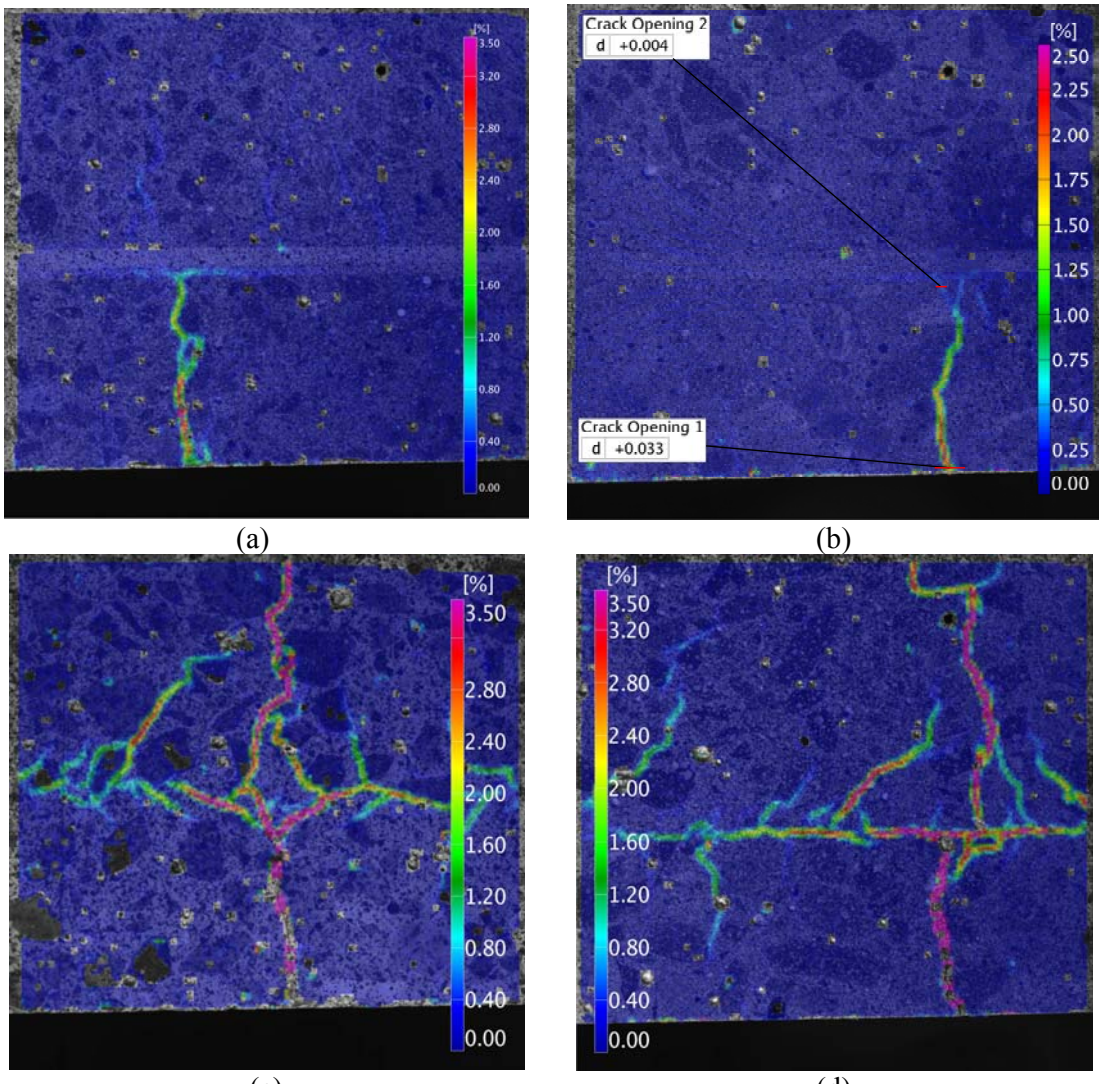

Figure 4: Computed Strain Overlay on Specimen with (a) 8 mm Maximum Aggregate Size under Estimated Cracking Load (14.0 kN) and with 16 mm Maximum Aggregate Size under (b) Estimated Cracking Load (13.0 kN), (c) 35.0 kN (single load), and (d) 35.0 kN (increasing cyclic load).

The computed strain in specimens with 8 mm and 16 mm maximum aggregate sizes while subjected to the estimated cracking load is shown in Figure 4(a) and 4(b), respectively. The transverse cracking propagates near aggregate interfaces and extends to the reinforcement; however, due to effect of the aggregate size the path of the cracks vary. The crack in the 8 mm maximum aggregate size specimen propagates completely around an aggregate and appears to be more tortuous than the crack in the larger aggregate size. In addition, the computed strain indicates that slight slip and/or separation occurs at the reinforcement/concrete interface even at these low load levels. Figure 4(c) shows the crack in a 16 mm maximum aggregate size specimen under 35.0 kN load. The transverse crack depth increases and extends past the reinforcement towards the neutral axis. The minimal slip and/or separation seen in Figures 4(a) and (b) has increased to extensive cracks which run parallel to the reinforcement. These cracks extend in both directions from the transverse crack in excess of 50 mm and beyond the measuring area. Figure 4(d) shows the cracking behavior in a 16 mm aggregate sample which was subjected to increasing cyclic loading (as discussed in Section 3.2). Although a non-uniform load level was applied, the effect of cyclic loading is still apparent when comparing Figure 4(c) with 4(d). After cyclic loading a continuous, nearly straight-line crack is seen at the reinforcement/concrete interface as opposed to the highly tortuous discontinuous cracking after a single load. The individual cracks seen in Figure 4(c) may therefore coalesce into a continuous crack under cyclic load, which would allow for a more rapid ingress of aggressive substances along the reinforcement. It should also be mentioned that the tortuous crack shown in Figure 4(a) had also coalesced after cyclic loading.

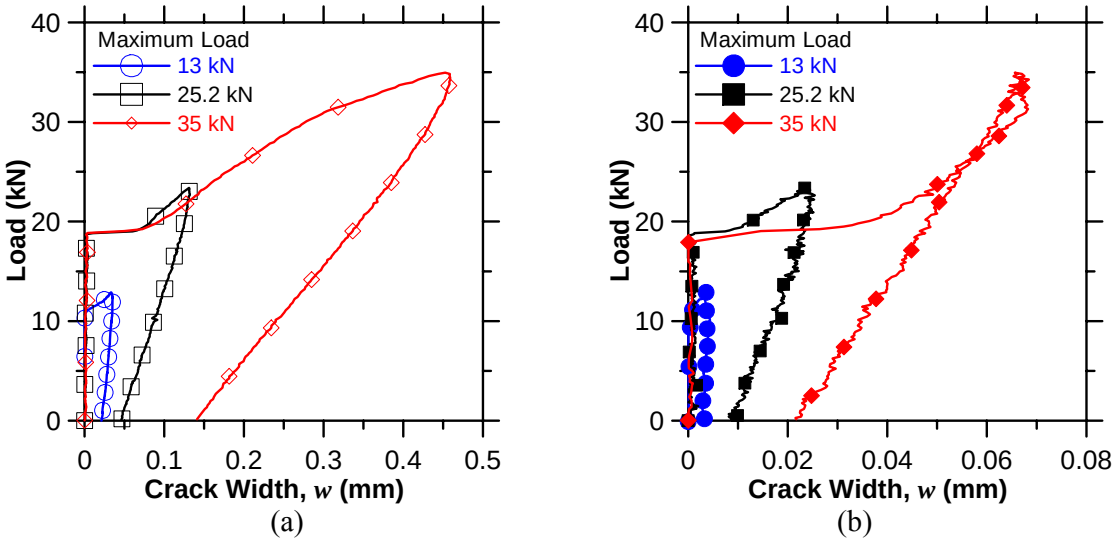

Figure 5: Transverse Cracking Response at Varying Loads in 16 mm Maximum Aggregate Size Specimen (a) at the Tension Face and (b) next to the Reinforcement.

Figure 4(b) shows an example of a point-point displacement measurements near the tension surface (Crack Opening 1) and near the reinforcement (Crack Opening 2). Additional point-point displacement measurements show the response at the reinforcement/concrete interface approximately 5 mm to the side of the transverse crack. Figure 5 shows the

transverse crack width as determined by a point-point displacement measurement versus the applied load for the 16 mm aggregate size specimen at varying load levels. The cracking at the tension face is shown in Figure 5(a) while the crack width near the reinforcement is seen in Figure 5(b). The crack width at the tensile face initiates at approximately 11 kN for the specimen loaded to 13.0 kN. The crack then opens rapidly to a maximum of 35 µm (it should be noted this crack was too small for visual observation during testing). The specimens loaded to higher levels cracked at higher loads, possible due to the increased loading rate. The crack widths at the tension face were measured by Aramis to be 0.13 mm and 0.46 mm at a load of 23.4 kN (1.8 times the estimated cracking load) and 35.0 kN, respectively. Figure 5(b) shows that the crack immediately propagates to the reinforcement and that the width at the reinforcement is significantly reduced compared to the crack width at the tensile face. Upon complete unloading, the crack remains open even near the reinforcement.

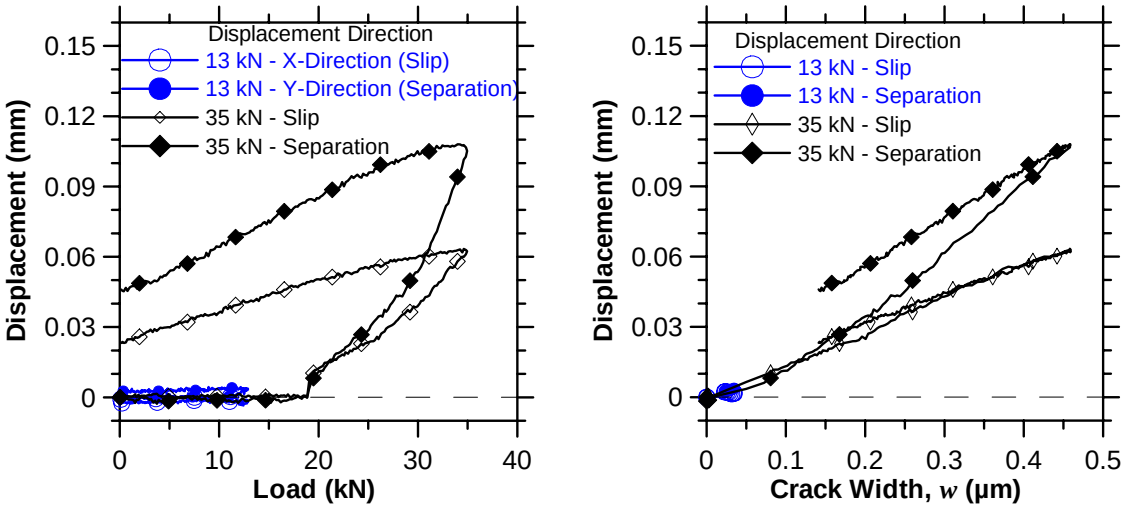

Figure 6: Cracking Response (i.e., Slip and Separation) at the Reinforcement/Concrete Interface versus (a) Load and (b) Crack Width at the Tension Face for 16 mm Maximum Aggregate Size Specimen.

Figure 4 showed that as the transverse crack reached the reinforcement cracking will continue parallel to the reinforcement. Therefore, point-point measurements were taken to determine the extent of this cracking. Figure 6 shows the corresponding slip and separation between the reinforcement and concrete due to increased flexural loading. Displacements were measured in the x-direction correspond to slip and the y-direction corresponding to separation. Figure 6(a) shows that separation between the reinforcement and concrete is effected more by the application of load resulting in a maximum separation of approximately 0.11 mm at 35.0 kN load. The slip is however also significant, reaching 0.06 mm at the extreme load level. At 13.0 kN, which resulted in a crack width at the tension face of only 36 µm, slip and separation also occurs, although to a minimal level (less the 5µm). Figure 6(b) shows the slip and separation as a function of the crack width at the tension face. Displacements at the reinforcement/concrete interface initiate and increase nearly immediately after cracking at the tensile face.

5. CONCLUSIONS

This paper has demonstrated that commercially available 3-D photogrammetry equipment may provide both qualitative and quantitative information on the cracking behavior of reinforced concrete. It has been shown that:

- While the strains shown by photogrammetric analysis are based upon deformation of facets in a computational mesh as opposed to actual material strain, the capability of visualizing cracks and measuring crack displacements prove quite useful.
- The strain data and point-point displacement measurements provide a means of creating a full field map of the cracking geometry and openings in reinforced concrete with a resolution of a few micrometer of crack opening. Such maps are essential for subsequent development of detailed models of cracking, ingress, and corrosion behavior. Furthermore, the effect of differences in material and loading characteristics on crack patterns may be visualized and quantified.
- Qualitative analysis of the computed strain overlay on a specimen image showed that the 8 mm aggregate specimens resulted in more tortuous cracks than the 16 mm aggregate specimen under single load applications, and that cracks coalesce into interconnected cracks under cyclic loading.
- Quantitative analysis of the cracking behavior showed that minimal cracking ($w \approx 35$ μm) at the tension face results in cracks near the reinforcement, which are not completely closed at unloading.
- Slip and separation between the reinforcement and concrete were found to develop and increase nearly immediately after transverse crack initiation at the tension face.
- Slip and separation along the reinforcement extend typically from approximately 10 mm to over 50 mm from the transverse crack depending on load level and number of load applications.

ACKNOWLEDGEMENTS

The authors gratefully acknowledge the support received from the Villam Kann Rasmussen Foundation to purchase the Aramis 3-D photogrammetry system. Additionally, the assistance of Lennart Østergaard with the Aramis system was instrumental to this work.

REFERENCES

[1] Virmani, Y.P. and Clemena, G.G., 'Corrosion Protection—Concrete Bridges,' *FHWA Report No. FHWA-RD-98-088* (September 1999).

[2] Koch, G.H., Brongers, M.P.H., Thompson, N.G., Virmani, Y.P., Payer, J.H., 'Corrosion Cost and Preventive Strategies in the United States,' *FHWA Report* (September 2001) (Available at www.corrosioncost.com).

[3] Wang, K., Jansen, D.C., Shah, S.P., and Karr, A.F., 'Permeability Study of Cracked Concrete,' *Cem. Concr. Res.* **27** (3) (1997) 381-393.

[4] Aldea, C.-M., Shah, S.P., and Karr, A., 'Permeability of Cracked Concrete,' Mater. Struct. **32** (June 1999) 370-376.

[5] De Schutter, G., 'Quantification of the Influence of Cracks in Concrete Structures on Carbonation and Chloride Penetration,' *Mag. Concr. Res.* **51** (6) (December 1999) 427-435.

[6] Rodriguez, O.G. and Hooton, R.D., 'Influence of Cracks on Chloride Ingress into Concrete,' *ACI Mater. J.* **100** (2) (March-April 2003) 120-126.
[7] Edvarson, C., 'Water Permeabiltiy and Autogenous Healing of Cracks in Concrete,' *ACI Mater. J.* **96** (4) (July-August 1999) 448-454.
[8] Jacobsen, S., Marchand, J., and Boisvert, L., 'Effect of Cracking and Healing on Chloride Transport in OPC Concrete,' *Cem. Concr. Res.* **26** (6) (1996) 869-881.
[9] Küter, A., Geiker, M.R., Olesen, J.F., Stang, H., Dauberschmidt, C., and Raupach, M., 'Chloride Ingress of Concrete Cracks under Cyclic Loading,' *Proc. ConMat'05* (Vancouver, BC, Canada) (August 22-24, 2005).
[10] Win, P.P, Watanabe, M., and Machida, A., 'Penetration Profile of Chloride Ions in Cracked Reinforced Concrete,' *Cem. Concr. Res.* **34** (2004) 1073-1079.
[11] Shah, S.P. and Weiss, W.J., 'High Strength Concrete: Strength, Permeability, and Cracking,' *Proc. PCI/FHWA Int. Symp. on HPC* (Orlando, Florida, 2000) 331-340.
[12] Weiss, W.J., Yang, W., and Shah, S.P., 'Factors Influencing Durability and Early-Age Cracking in High-Strength Concrete Structures,' *ACI SP-189 High Per. Concr.: Res. to Practice* (January 2000) 387-410.
[13] Darwin, D., Browning, J., and Lindquist, W.D., 'Control of Cracking in Bridge Decks: Observations from the Field,' *Cem. Concr. Agg.* **26** (2) (December 2004) 148-154.
[14] Schieβl, P., and Raupach, M., 'Laboratory Studies and Calculations on the Influence of Crack Width on Chloride-Induced Corrosion of Steel in Concrete,' *ACI Mater. J.* **94** (1) (January-February 1997) 56-62.
[15] Mohammed, T.U., Otsuki, N., Hisada, M., and Shibata, T., 'Effect of Crack Width and Bar Type on Corrosion of Steel in Concrete,' *J. Mater. Civil Engng.* **13** (3) (2001) 194-201.
[16] Marcotte, T.D. and Hansson, C.M., 'The Influence of Silica Fume on the Corrosion Resistance of Steel in High Performance Concrete Exposed to Simulated Sea Water,' *J. Mater. Sci.* **28** (2003) 4765-4776.
[17] Berke, N.S., Dallaire, M.C., Hicks, M.C., and Hoopes, R.J., 'Corrosion of Steel in Cracked Concrete,' *Corrosion Engineering* **49** (11) (1993) 934-943.
[18] Arya, A., and Ofori-Darko, F.K., 'Influence of Crack Frequency on Reinforcement Corrosion in Concrete,' *Cem. Concr. Res.* **26** (3) (1996) 345-353.
[19] Yang, Z., 'Assessing Cumulative Damage in Concrete and Quantifying its Influence on Life Cycle Performance Modeling,' *Ph.D. Thesis* (Purdue University, West Lafayette, IN) (2004).
[20] GOM Optical Measuring Techniques, 'Aramis v5.4 User Manual,' *GOM mbH* (2005) (www.gom.com).